Synthesis of five isostructural tetranuclear Fe_2Ln_2 (Ln = Gd, Tb, Dy, Ho, Er) complexes with an "inverse butterfly" core

Ghulam Abbas [a], Masooma Ibrahim [b], Sebastian F.M. Schmidt [a], Eufemio Moreno-Pineda [b], Christopher E. Anson [a], Annie K. Powell [a,b,*]

[a] Institute of Inorganic Chemistry, Karlsruhe Institute of Technology, Engesserstrasse 15, 76131 Karlsruhe, Germany
[b] Institute of Nanotechnology, Karlsruhe Institute of Technology, Hermann von-Helmholtz Platz 1, 76344 Eggenstein-Leopoldshafen, Germany

ABSTRACT

A one-pot synthesis leading to in situ ligand formation enabled the preparation of five isostructural tetranuclear Fe_2Ln_2 coordination clusters $[Fe_2Ln_2(\mu_4L)_2(mpm)_2(piv)_2(N_3)_{4-x}(Cl)_x]$, where H_2L is 2-((pyridin-2-ylmethylene)amino)propan-1,3-diol, Hmpm is methoxy(2-pyridinyl)methanol, piv is pivalate and Ln = Gd (**1**), Tb (**2**), Dy (**3**), Ho (**4**) and Er (**5**). These show an unprecedented core structure. The coordination compounds were fully characterised by infrared spectroscopy, elemental analysis, powder X-ray diffraction and single crystal X-ray diffraction. Magnetic measurements indicate the presence of intramolecular antiferromagnetic and ferromagnetic interactions. The finding is important in developing synthetic strategies for the preparation of new molecular based magnetic materials.

1. Introduction

Heterometallic 3d-4f complexes with butterfly cores are of immense interest to synthetic chemists due to their potential applications as luminescent [1–3], catalytic [4,5] as well as magnetic materials [6]. Heterometallic complexes have also been investigated as single molecule magnets (SMMs), molecules that retain magnetisation even after an external magnetic field has been turned off [7–12]. The prerequisite for SMMs include a large uniaxial magnetoanistropy and non-zero spin state which result in a significant magnetisation energy barrier at low temperatures [13,14]. 3d-4f metal complexes can display enhanced relaxation properties due to the magnitude of spin and spin-orbital coupling based anisotropy by 4f metal ions [15]. The majority of the 3d-4f compounds with a butterfly core have the 3d metals in the body positions and the lanthanides in the wingtips [16,17]. Although there are several examples of this inverted topology for $Cr_2^{III}Ln_2$, $Co_2^{III}Ln_2$ and $Ru_2^{III}Ln_2$ compounds [18–22], in the case of Fe_2Ln_2, there is only one previous example where the lanthanides are in the body positions and iron is in the wingtips [23]. In the standard situation strong antiferromagnetic coupling between the iron ions is observed.

In the reverse case we expect weak Ln–Ln and Fe–Ln interactions, where the interactions between the 4f metals are expected to be lower than the 3d-4f interactions (Fig. 1).

We report here the synthesis and magnetic properties of tetranuclear isostructural $[Fe_2Ln_2(\mu_4-L)_2(mpm)_2(piv)_2(N_3)_4]$ complexes containing a Schiff base ligand displaying a unique deformed butterfly core; (H_2L) = 2-((pyridin-2-ylmethylene)amino)propan-1,3-diol, Hmpm = methoxy(2-pyridinyl)methanol, piv = pivalate and Ln = (Gd, Tb, Dy, Ho, Er) (Scheme 1). To the best of our knowledge the coordination chemistry of H_2L has not been explored up to now. Moreover, the methoxy(2-pyridinyl)methanolate is generated in situ and displays chelating/bridging coordination modes for assembling Fe_2Ln_2 complexes in good yields. The phase purity was checked by powder XRD. Furthermore, we will highlight how the presence of the four μ_3-OR and two (μ_2-OR) bridges in the unique butterfly core can tune the magnetic properties in these Fe_2Ln_2 complexes.

2. Experimental

2.1. Materials and methodology

All reagents were obtained from commercial sources and were used as received without further purification unless otherwise stated. All reactions were carried out under aerobic conditions. The

* Corresponding author at: Institute of Inorganic Chemistry, Karlsruhe Institute of Technology, Engesserstrasse 15, 76131 Karlsruhe, Germany.
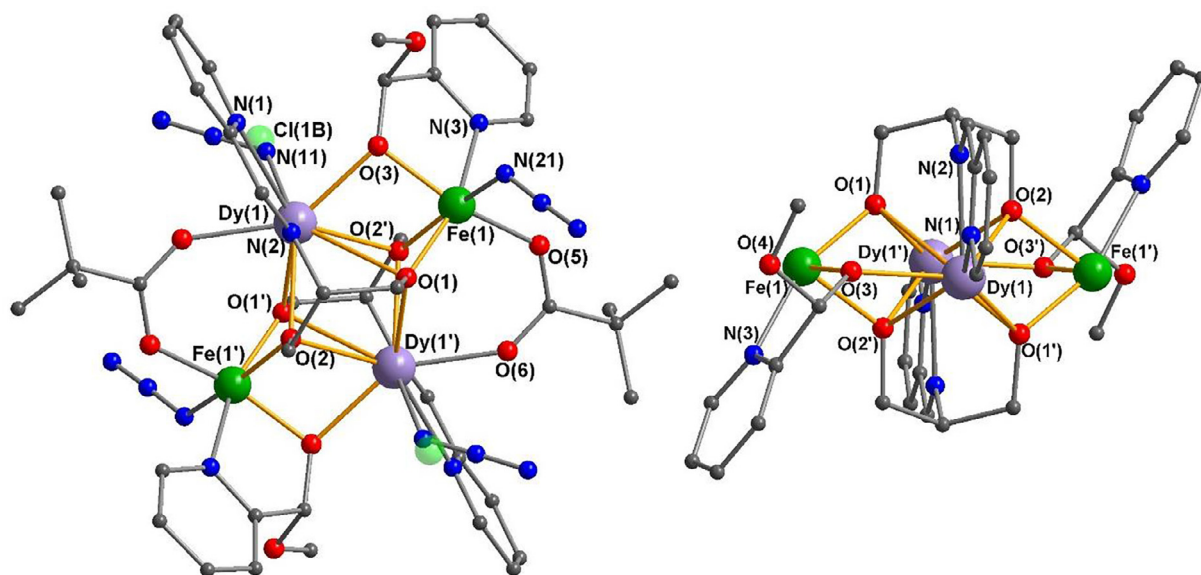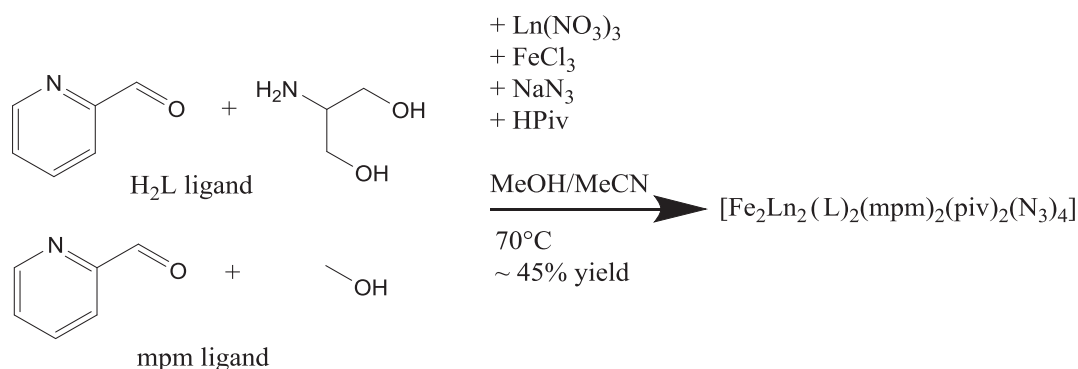 *E-mail address:* annie.powell@kit.edu (A.K. Powell).

Fig. 1. Left: Molecular structure of **3**. Colour code: Dy purple Fe green; O red; N blue; C gray; Cl pale green. All H atoms have been omitted for clarity. Right: Core structure, Azide and pivalate ligands omitted for clarity. (Color online.)

Scheme 1. *In situ* conversion of picolinaldehyde into methoxy(2-pyridinyl)methanol and synthesis of 2-((pyridin-2-ylmethylene)amino) propan-1,3-diol (H₂L).

elemental analyses (C, H, N) were performed at the Institute of Inorganic Chemistry (KIT) using an Elementar Vario EL analyzer. Fourier transform IR spectra were measured on a Perkin–Elmer Spectrum One spectrometer with samples prepared as KBr discs. X-ray powder diffraction patterns were measured at room temperature using a Stoe STADI-P diffractometer with a Cu Kα radiation.

2.2. Synthesis of the complexes

2.2.1. Synthesis of $[Fe_2Gd_2(\mu_4L)_2(mpm)_2(piv)_2(Cl)_{0.5}(N_3)_{3.5}]$ (**1**)

The same procedure was employed to prepare all complexes and hence only the compound **1** is described here in detail. A solution of pyridine-2-carboxyaldehyde (160 mg, 1.5 mmol) and 2-amino-1,3-propanediol (104 mg, 1.5 mmol) in MeOH (15 mL) was stirred for 30 min at 70 °C, followed by the addition of Gd(NO₃)₃·6H₂O (112 mg, 0.25 mmol), FeCl₃ (40 mg, 0.25 mmol), NaN₃ (51 mg, 0.75 mmol) and pivalic acid (77 mg, 0.75 mmol) in MeCN (15 mL). The mixture was heated under reflux for 1 h after which it was cooled to room temperature and then allowed to stand undisturbed in a sealed vial. Orange needles of **1** suitable for X-ray crystallography were obtained after 2 days. The crystals of **1** were collected by filtration, washed with MeCN and dried in vacuum.

Yield: 74 mg, ~42%. *Anal.* Calc. for $C_{42}H_{54}Cl_{0.5}Fe_2Gd_2N_{16.5}O_{12}$ (**1**): C, 35.38; H, 3.82; N, 16.21. Found: C, 35.15; H, 3.78; N, 16.26%. IR (KBr): ν (cm⁻¹) = 3648 (w), 2963 (w), 2533 (w), 2364 (s), 2163 (w), 2035 (w), 1771 (w) 1720 (m), 1701 (vs), 1684 (m), 1653 (vs), 1561 (vs), 1542 (s), 1523 (m), 1507 (m), 1476 (m), 1459 (m), 1418 (s), 1100 (w), 1057 (m), 989 (m), 951 (w) 883 (w), 774 (w), 671 (m), 586 (m), 421 (w).

Yield: 82 mg, ~46%. Anal. Calc. for $C_{42}H_{54}Tb_2Fe_2N_{18}O_{12}$ (**2**): C, 35.21; H, 3.78; N, 17.60. Found: C, 35.06; H, 3.75; N, 17.35%. IR (KBr): ν (cm⁻¹) = 3650 (w), 2965 (w), 2533 (w), 2364 (s), 2163 (w), 2035 (w), 1773 (w) 1717 (m), 1701 (vs), 1687 (m), 1653 (vs), 1563 (vs), 1540 (s), 1519 (m), 1507 (m), 1476 (m), 1457 (m), 1420 (s), 1100 (w), 1059 (m), 991 (m), 951 (w) 883 (w), 774 (w), 671 (m), 588 (m), 421 (w).

Yield: 80 mg, ~45%. Anal. Calc. for $C_{42}H_{54}Dy_2Fe_2N_{18}O_{12}$ (**3**): C, 35.04; H, 3.78; N, 17.51. Found: C, 35.13; H, 3.62; N, 17.42% IR (KBr): ν (cm-1) = 3649 (w), 2961 (w), 2962 (w), 2362 (w), 2161 (w), 2034 (w), 1771 (w) 1722 (m), 1699 (vs), 1684 (m), 1653 (vs), 1558 (vs), 1547 (m), 1517 (s), 1507 (m), 1478 (m), 1457 (m), 1418 (w), 1061 (m), 993 (w), 883 (w), 776 (w), 671 (w), 586 (m), 417 (w).

Yield: 77 mg, ~43%. Anal. Calc. for $C_{42}H_{54}Cl_{0.7}Ho_2Fe_2N_{15.9}O_{12}$ (**4**): C, 35.03; H, 3.78; N, 15.47. Found: C, 35.01; H, 3.80; N, 15.55%; IR (KBr): ν (cm⁻¹) = 3648 (w), 2963 (w), 2533 (w), 2362
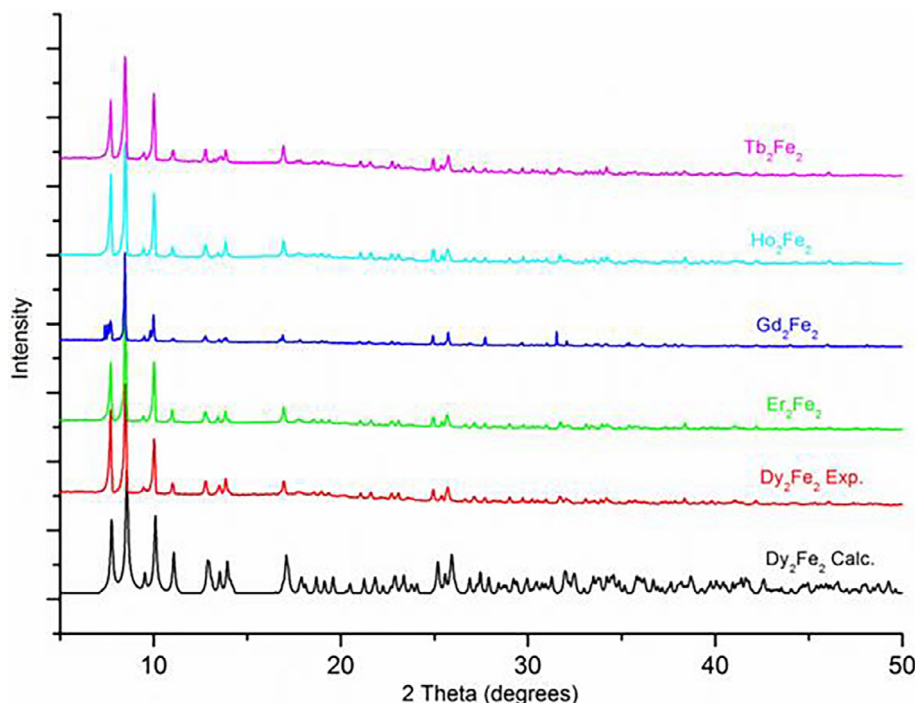
Fig. 2. Comparison of PXRD patterns of $[Fe_2Ln_2(\mu_3\text{-}O)_4(H_2L)_2(mpm)_2(Piv)_2(N_3)_4]$ series.

(s), 2166 (w), 2035 (w), 1773 (w), 1724 (m), 1699 (vs), 1684 (m), 1656 (vs), 1563 (vs), 1542 (s), 1519 (m), 1507 (m), 1476 (m), 1459 (m), 1420 (s), 1100 (w), 1059 (m), 989 (m), 951 (w) 883 (w), 776 (w), 671 (m), 588 (m), 421 (w).

Yield: 80 mg, ∼45%. *Anal.* Calc. for $C_{42}H_{54}Cl_{0.3}Er_2Fe_2N_{17.1}O_{12}$ (**5**): C, 34.86; H, 3.76; N, 16.55. Found: C, 34.70; H, 3.72; N, 16.64% IR (KBr): ν (cm^{-1}) = 3650 (w), 2963 (w), 2535 (w), 2362 (s), 2162 (w), 2035 (w), 1775 (w), 1724 (m), 1699 (vs), 1684 (m), 1653 (vs), 1563 (vs), 1540 (s), 1521 (m), 1507 (m), 1474 (m), 1457 (m), 1424 (s), 1100 (w), 1059 (m), 989 (m), 951 (w) 883 (w), 776 (w), 671 (m), 584 (m), 421 (w).

2.3. Magnetic measurements

Magnetic susceptibility measurements were obtained using a Quantum Design SQUID magnetometer (MPMS-XL). Measurements were performed on polycrystalline samples of **3**. ac susceptibility measurements were measured with an oscillating ac field of 3 Oe and a frequency ranging from 1 and 1500 Hz. The magnetic data were corrected for the sample holder.

2.4. X-ray crystallography

Data on a single crystal of **3** were collected at 180 K on a Stoe IPDS II area detector diffractometer using graphite-monochromated Mo Ka radiation. Semi-empirical absorption corrections were applied using XPREP in SHELXTL. The structure was solved using direct methods SHELXT, followed by full-matrix least-squares refinement against F^2 (all data) using SHELXTL in Olex2 [24,25]. Anisotropic refinement was used for all non-H atoms except the minor-occupancy chlorine atom; organic H atoms were placed in calculated positions. The structures of compounds 1,2,4 and 5 were established by determining the unit cell parameters on single crystals (Table 2) and collecting X-ray powder diffraction patterns (Fig. 2). The data presented in Table 2 and Fig. 2 support the suggestion that all the compounds are isomorphous. Powder X-ray diffraction data were measured at ambient temperature on a Stoe

Table 1
Crystallographic data and structure refinement for compound **3**.

	3
Formula	$C_{42}H_{54}Cl_{0.22}Dy_2Fe_2N_{17.34}O_{12}$
Mr	1438.28
Crystal size [mm]	0.19 × 0.16 × 0.13
Color	Red block
Cryst system	monoclinic
Space group	$P2_1/c$
T [K]	180
a [Å]	11.9953(11)
b [Å]	15.9653(12)
c [Å]	14.2198(15)
α [°]	90
β [°]	108.282(8)
γ [°]	90
V [Å^3]	2585.8(4)
Z	2
ρ_{calcd} [g cm^{-3}]	1.847
μ (Mo Kα) [mm^{-1}]	3.494
F(0 0 0)	1422
Reflections collected	20,951
Unique reflections	5479
R_{int}	0.0758
Reflections observed [$I > 2\sigma(I)$]	4231
Parameters/restraints	351/27
Goodness-of-fit (GOF) on F^2	1.014
R_1 [$I > 2\sigma(I)$]	0.0259
wR_2 (all data)	0.0438
Largest residuals [e Å^{-3}]	+1.16/ −2.02
CCDC number	1842066

STADI-P diffractometer with a Cu Kα radiation at the Institute of Nanotechnology, Karlsruhe Institute of Technology.

3. Results and discussion

3.1. Synthetic comments

The Schiff base and methoxy(pyridinyl)methanol ligands were prepared in situ in MeOH solution prior to the addition of Ln
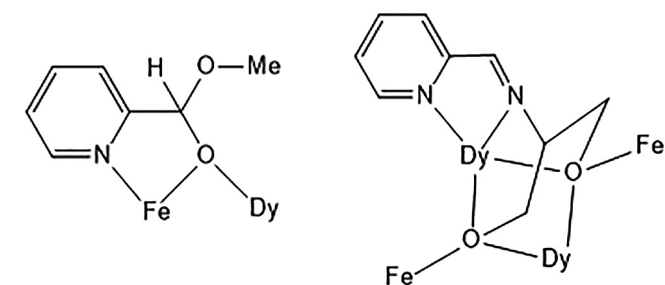
Table 2
Unit cells for compounds **1**–**5**.

Formula	**1** (Gd)	**2** (Tb)	**3** (Dy)	**4** (Ho)	**5** (Er)
a [Å]	11.9986(12)	12.07(3)	11.9953(11)	12.059(10)	12.0485(6)
b [Å]	15.8525(15)	16.01(3)	15.9653(12)	15.972(12)	15.9616 (7)
c [Å]	14.414(2)	14.38(3)	14.2198(15)	14.395(11)	14.0986 (4)
α [°]	90	90	90	90	90
β [°]	108.269(12)	107.82(19)	108.282(8)	108.29(7)	108.110
γ [°]	90	90	90	90	90
V [Å^3]	2603.5(6)	2646(9)	2585.8(4)	2633(4)	2577.02 (9)

$(NO_3)_3 \cdot 6H_2O$, $FeCl_3$, NaN_3 and pivalic acid in a molar ratio of (1:1:3:3) in MeCN. The reaction mixture was refluxed which fosters the synthesis of compounds (**1**–**5**) in the absence of any base. Several reactions were performed with different solvents and using different ratios and other conditions before the successful procedures were identified. Furthermore the use of only a protic solvent such as MeOH, or a mixture of $MeOH/CH_2Cl_2$, also leads to different, as yet unidentified, products.

3.2. Crystal structure of $[Fe_2Dy_2(\mu_4L)_2(mpm)_2(piv)_2(N_3)_{3.78}(Cl)_{0.22}]$ (**3**)

X-ray powder diffraction indicated that all five compounds in the series were isomorphous (Fig. 2); the full structure of **3** was determined by single-crystal X-ray diffraction (Table 1). The coordination clusters, possessing an inverse-butterfly core, are formulated as $[Fe_2Ln_2(\mu_4L)_2(mpm)_2(piv)_2(N_3)_{4-x}(Cl)_x]$ where Ln = Gd (**1**), Tb (**2**), Dy (**3**), Ho (**4**) and Er (**5**). The Dy^{III} centres occupy the body sites whereas Fe^{III} centres are at the wingtip positions. The single-crystal X-ray structure of **3** showed that it crystallizes in

Scheme 2. Bridging modes of η^1:η^1:μ_2 methoxy(2-pyridinyl)methanolate (mpm)$^-$ and of ligand L^{2-}.

the monoclinic space group $P2_1/c$ with $Z = 2$. As mentioned above, compounds **1**–**5** are isomorphous and thus can be compared with the molecular structure of **3** which has a crystallographically centrosymmetric $[Fe_2^{III}Dy_2^{III}(\mu_3\text{-}OR)_4]$ core. The tetranuclear cores of all compounds are held together by four μ_3-OR bridges from the two chelating/bridging (μ_4-L)$^{2-}$ ligands, two chelating/bridging (μ_2-mpm) ligands, two bidentate (η^1:η^1:μ_2) pivalates (Scheme 2), together with four unidentate azides. Selected bond lengths and angles of compound **3** are given in Table 3.

Atoms Dy(1) and Dy(1′) (see Table 3) occupy the body sites, and Fe(1) and Fe(1′) occupy the wingtips of the "inverse-butterfly" topology. The central $[Fe_2^{III}Dy_2^{III}(\mu_3\text{-}OR)_4]$ core can be also described as two edge-sharing $[FeDy_2(\mu_3\text{-}OR)_2]$ triangular subunits, in which the four metal ions are coplanar, with the (μ_3-OR)$_2$ units above and below the Fe_2Dy_2 plane (by 1.698, 1.855 Å). The (μ_2-OR) bridges from the (mpm)$^-$ ligands result in each $FeDy_2$ triangle being scalene (and almost isosceles), with the μ_2-bridged Fe(1)-Dy(1) edge being shorter (3.2752(5) Å) than the other two (3.5391(5) and 3.5616(6) Å). .The tetranuclear cores are well isolated within the crystal structure, exhibiting no supramolecular interactions such as hydrogen bonding between adjacent entities. A literature survey reveals that tetranuclear Fe_2Ln_2 coordination clusters with a coplanar Fe_2Ln_2 core often have a symmetrical butterfly topology [10–15]. Due to the two μ_2-OR bridges in **3**, its core deviates from a symmetrical inverse-butterfly core to a deformed inverse-butterfly. The coordination number of the Fe^{III} ions is six, with a FeO_4N_2 environment having distorted octahedral geometry, whereas the coordination number of Dy^{III} is nine with a DyO_6N_3 distorted monocapped square antiprismatic geometry.

3.3. Magnetic properties of **1**–**5**

The magnetic susceptibilities of the complexes **1**–**5** were measured on polycrystalline samples over the temperature range

Table 3
Selected bond angles and bond lengths of compound **3**.

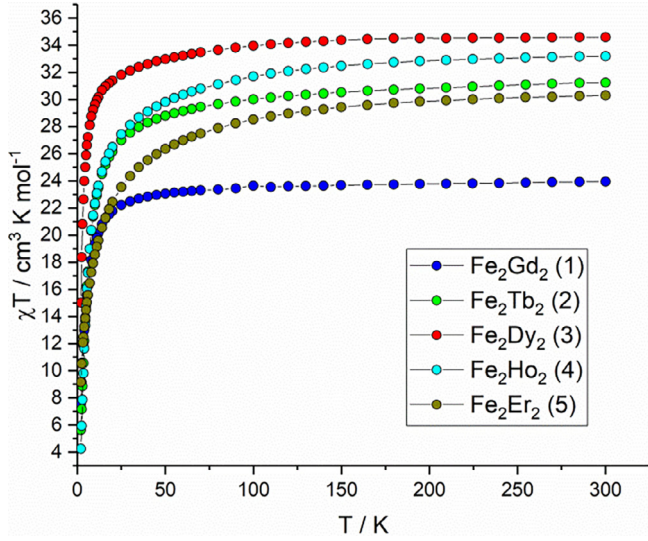| Atom1	Atom2	Distance (Å)	Atom12	Atom23	Distance (Å)4
Dy1	N1	2.695(2)	Fe1	O1	1.9800(19)
Dy1	O2	2.4482(18)	Fe1	O2	2.0828(19)
Dy1	O1	2.7512(19)	Fe1	O3	1.9924(19)
Dy1	N2	2.428(2)	Fe1	O5	1.995(2)
Dy1	N11	2.355(6)	Fe1	N3	2.184(2)
Dy1	O1	2.4086(19)	Fe1	N21	1.989(3)
Dy1	O6	2.3072(19)	Dy1	Fe1	3.2752(5)
Dy1	O3	2.3217(19)	Dy1	Fe1	3.5616(6)
Dy1	O2	2.4509(18)	Dy1	Dy1	3.5391(5)
Atom1	Atom2	Atom3	Angle (°)		
Fe1	O1	Dy1	108.10(8)		
Fe1	O2	Dy1	103.25(7)		
Fe1	O3	Dy1	98.50(8)		
Fe1	O1	Dy1	85.99(7)		
Fe1	O2	Dy1	92.22(7)		
Dy1	O1	Dy1	86.35(6)		
Dy1	O2	Dy1	92.51(6)		

Fig. 3. χT vs T of complexes **1**–**5**.

2 – 300 K (Fig. 3). The results are summarised in Table 4. In all five compounds the room temperature value of χT is in a good agreement with the expected value for two uncoupled Fe^{3+} ions and the two respective uncoupled lanthanide ions. For all five lanthanides the χT product remains roughly constant down to a temperature of about 40 K. This is indicative of weak interactions, as is expected from the crystal structure, where bridging atoms exist only between the lanthanides or between the lanthanides and Fe^{3+}. Since the 4f electrons responsible for the magnetic coupling of the lanthanides are well shielded any magnetic interaction involving lanthanides is usually weak. From 40 K the χT product of all lanthanides drops steadily. This behavior is caused by a combination of the depopulation of M_J sub-levels with decreasing temperature and the magnetic interactions.

In order to better understand the interactions between the paramagnetic centres the χT product of Fe_2Gd_2 (**1**) was fitted to the following spin Hamiltonian which corresponds to the spin model displayed in Fig. 4. We chose a three J Hamiltonian to take the significantly different Fe^{3+} – Gd^{3+} distances within the butterfly into account. **1** was used because Gd^{3+} has, in contrast to the other lanthanide ions used in this study, no orbital momentum [21] Fig. 5.

$$H = -2J_1\left(S\left(Gd^{3+}\right)S\left(Gd^{3+}\right)\right) - 2J_2 2\left(S\left(Gd^{3+}\right) * S\left(Fe^{3+}\right)\right)$$
$$- 2J_3 2\left(S\left(Gd^{3+}\right) * S\left(Fe^{3+}\right)\right) + 2g\mu_B S\left(Fe^{3+}\right) + 2g\mu_B S\left(Gd^{3+}\right)$$

The best fit was obtained with a J1 of 0.20 cm^{-1}, J2 of 0.19 cm^{-1} and a J3 of 0.14 cm^{-1}. In our inverse-butterfly topology there is no direct superexchange path between the two Fe^{3+} ions, so that this magnetic interactions is negligible, whereas in Fe/4f

compounds such interactions usually dominate. The magnitudes of the interactions between Fe^{3+} and Gd^{3+} are in line with values found in the literature [26]. Although a few examples of butterfly structures with a similar topology can show stronger magnetic interactions between the Ln^{3+} and Fe^{3+}, and magnetic hysteresis up to 4 K, in our case the magnetic interactions are weaker, and the combination of both antiferromagnetic and ferromagnetic interactions within the Fe_2Gd_2 core can result in a non-frustrated S = 0 ground state [27]. However the magnetic behaviour of the anisotropic Fe_2Dy_2 (**3**) analogue (Fig. 6) may be more complex.

The Magnetisation versus Field plot shows an inflection at about 0.8 T and 2 K (Fig. 6). This is not an unusual behavior in 3d4f compounds and indicates a magnetic level crossing [28,29]. This behavior can only be rationalized in the scope of an interplay of the spin topology and the anisotropy of the Dy^{3+} ions.
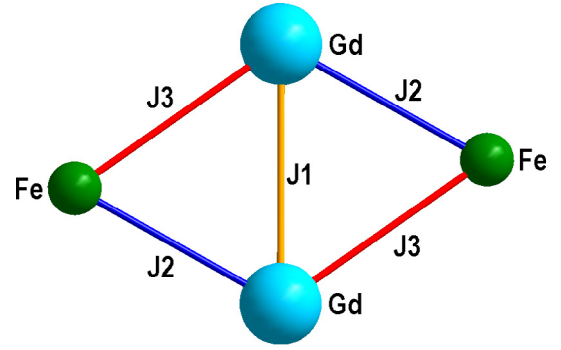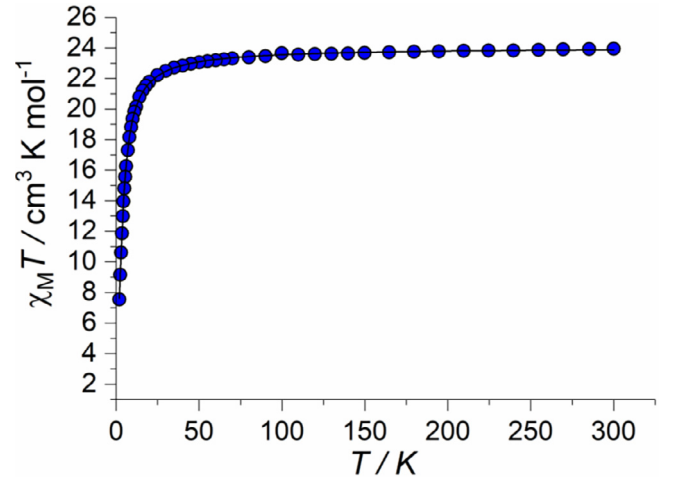

Fig. 4. Spin model used for the fitting of Fe_2Gd_2 (**1**).

Fig. 5. χT vs T of complex **1**. The black line corresponds to the results of the fitting.

Table 4
Magnetic data extracted from χT vs T for compounds **1**–**5**.

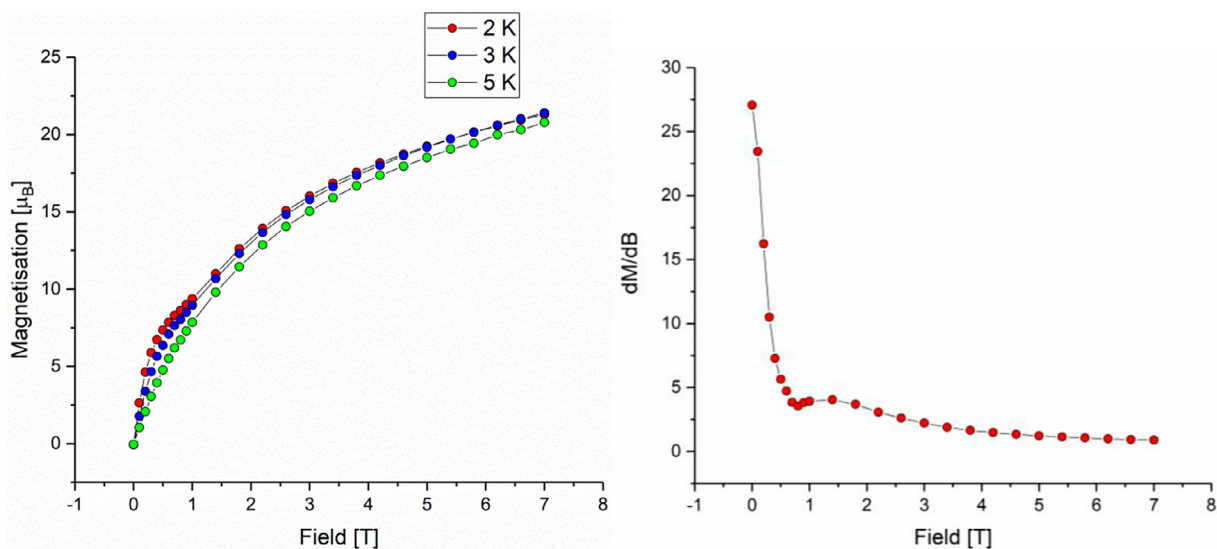| Compounds	Ground state of the Ln^{3+} ion	Curie Constant for each Ln ion at 300 K (cm^3 K/mol)	χT (cm^3 K/mol) at 300 K, calc. from Curie constants	χT (cm^3 K/mol) at 300 K	χT (cm^3 K/mol) at 2 K
Fe_2Gd_2 (**1**)	$^8S_{7/2}$	7.87	24.49	23.94	7.54
Fe_2Tb_2 (**2**)	$^7S_6$	11.82	32.39	31.25	5.63
Fe_2Dy_2 (**3**)	$^6H_{15/2}$	14.17	37.09	34.58	15.02
Fe_2Ho_2 (**4**)	$^5I_8$	14.07	36.89	33.17	4.25
Fe_2Er_2 (**5**)	$^4I_{15/2}$	11.48	31.71	30.29	9.15

Fig. 6. Left: Magnetisation vs Field at 2, 3 and 5 K of compound **3** Fe_2Dy_2 Right: First derivative of the magnetisation vs applied Field at 2 K.

4. Conclusion

Using an in situ synthetic strategy we were able to produce Fe_2Ln_2 inverse-butterfly compounds with the rare "wing/body swapping" feature in which the body positions are occupied by the Ln^{3+} ions and the wingtips by the Fe^{3+} ions. Another feature of this core structure is that the two bridging RO^- groups result in longer and shorter Gd^{3+}-Fe^{3+} distances. Fitting of the magnetic data for the Gd^{3+} analogue reveals that the absolute values of the superexchange parameters are all of similar magnitude, but while the Gd-Gd and one of the Fe-Gd interactions are antiferromagnetic, the other Fe-Gd is ferromagnetic, probably resulting in a S = 0 ground state. This spin topology, in combination with the anisotropy of the Dy^{3+} ion, then results in a level crossing phenomenon.

Acknowledgements

References

[1] I. Oyarzabal, B. Artetxe, A. Rodríguez-Diéguez, J.Á. García, J.M. Seco, E. Colacio, A family of acetato-diphenoxo triply bridged dimetallic $Zn^{II}Ln^{III}$ complexes: SMM behavior and luminescent properties, Dalton Trans. 45 (2016) 9712, https://doi.org/10.1039/c6dt01327a.

[2] C.Y. Chow, S.V. Eliseeva, E.R. Trivedi, T.N. Nguyen, V.L. Pecoraro, Ga^{3+}/Ln^{3+} metallacrowns: a promising family of highly luminescent lanthanide complexes that covers visible and near-infrared domains, J. Am. Chem. Soc. 138 (2016) 5100, https://doi.org/10.1021/jacs.6b00984.

[3] Y. Lu, X.-M. Jiang, S.-D. Zhu, Z.-Y. Du, C.-M. Liu, Y.-R. Xie, L.-X. Liu, Anion effects on lanthanide(III) tetrazole-1-acetate dinuclear complexes showing slow magnetic relaxation and photofluorescent emission, Inorg. Chem. 55 (2016) 3738, https://doi.org/10.1021/acs.inorgchem.5b02432.

[4] K. Griffiths, K. Griffiths, P. Kumar, G.R. Akien, N.F. Chilton, A. Abdul-Sada, G.J. Tizzard, S.J. Coles, G.E. Kostakis, Tetranuclear Zn/4f coordination clusters as highly efficient catalysts for Friedel-Crafts alkylation, Chem. Commun. 52 (2016) 7866, https://doi.org/10.1039/C6CC03608B.

[5] P. Kumar, S. Lymperopoulou, K. Griffiths, S. Sampani, G.E. Kostakis, Highly efficient tetranuclear $Zn_2^{II}Ln_2^{III}$ catalysts for the Friedel-Craft alkylation of indoles and nitrostyrenes, Catalysts 6 (2016) 140, https://doi.org/10.3390/catal6090140.

[6] E. Moreno-Pineda, N.F. Chilton, F. Tuna, R.E.P. Winpenny, E.J.L. McInnes, Systematic study of a family of butterfly-like Mn_2Ln_2 molecular magnets (M = Mg^{II}, Mn^{II}, Co^{II}, Ni^{II} and Cu^{II}; Ln = Y^{III}, Gd^{III}, Tb^{III}, Dy^{III}, Ho^{III} and Er^{III}), Inorg. Chem. 54 (2015) 5930, https://doi.org/10.1021/acs.inorgchem.5b01761.

[7] R. Sessoli, D. Gatteschi, A. Caneschi, M.A. Novak, Magnetic bistability in a metal-ion cluster, Nature 365 (1993) 141, https://doi.org/10.1038/365141a0.

[8] R. Sessoli, H.-L. Tsai, A.R. Schake, S. Wang, J.B. Vincent, K. Folting, D. Gatteschi, G. Christou, D.N. Hendrickson, High spin molecules:[$Mn_{12}O_{12}(O_2CR)_{16}(H_2O)_4$], J. Am. Chem. Soc. 115 (1993) 1804.

[9] C.D. Polyzou, A. Baniodeh, N. Magnani, V. Mereacre, N. Zill, C.E. Anson, S.P. Perlepes, A.K. Powell, Squashed $Fe_2^{III}M_4^{III}$ octahedra (M = Y, Gd, Dy) from the first use of the cyanoacetate ligand in 3d/4f coordination chemistry, RSC Adv. 5 (2015) 10763, https://doi.org/10.1039/C4RA15458D.

[10] D. Dermitzaki, C.P. Raptopoulou, V. Psycharis, A. Escuer, S.P. Perlepes, T.C. Stamatatos, Nonemployed simple carboxylate ions in well-investigated areas of heterometallic carboxylate cluster chemistry: a new family of $Cu(II)_4Ln(III)_8$ complexes bearing tert-butylacetate bridging ligands, Inorg. Chem. 54 (2015) 7555, https://doi.org/10.1021/acs.inorgchem.5b01179.

[11] C.J. Milios, A. Vinslava, W. Wernsdorfer, S. Moggach, S. Parsons, S.P. Perlepes, G. Christou, E.K. Brechin, A record anisotropy barrier for a single-molecule magnet, J. Am. Chem. Soc. 129 (2007) 2754, https://doi.org/10.1021/ja068961m.

[12] N.C. Anastasiadis, D.A. Kalofolias, A. Philippidis, S. Tzani, C.P. Raptopoulou, V. Psycharis, C.J. Milios, A. Escuer, S.P. Perlepes, A family of dinuclear lanthanide (III) complexes from the use of a tridentate Schiff base, Dalton Trans. 44 (2015) 10200, https://doi.org/10.1039/c5dt01218j.

[13] D. Gatteschi, R. Sessoli, Quantum tunneling of magnetization and related phenomena in molecular materials, Angew. Chem. Int. Ed. Engl. 42 (2003) 268.

[14] S.T. Liddle, J. van Slageren, Improving f-element single molecule magnets, Chem. Soc. Rev. 44 (2015) 6655, https://doi.org/10.1039/c5cs00222b.

[15] J.D. Rinehart, M. Fang, W.J. Evans, J.R. Long, Strong exchange and magnetic blocking in N_2^3-radical-bridged lanthanide complexes, Nat. Chem. 3 (2011) 538, https://doi.org/10.1038/nchem.1063.

[16] K.C. Mondal, A. Sundt, Y. Lan, G.E. Kostakis, O. Waldmann, L. Ungur, L.F. Chibotaru, C.E. Anson, A.K. Powell, Coexistence of distinct single-ion and exchange-based mechanisms for blocking of magnetization in a $Co_2^{II}Dy_2^{III}$ single-molecule magnet, Angew. Chem., Int. Ed. Engl. 51 (2012) 7550, https://doi.org/10.1002/anie.201201478.

[17] A. Baniodeh, V. Mereacre, N. Magnani, Y. Lan, J.A. Wolny, V. Schünemann, C.E. Anson, A.K. Powell, Para versus meta ligand substituents as a means of directing magnetic anisotropy in Fe_2Dy_2 coordination clusters, Chem. Commun. 49 (2013) 9666, https://doi.org/10.1039/c3cc45695a.

[18] S.K. Langley, D.P. Wielechowski, V. Vieru, N.F. Chilton, B. Moubaraki, B.F. Abrahams, L.F. Chibotaru, K.S. Murray, A $Cr_2^{III}Dy_2^{III}$ single-molecule magnet: Enhancing the blocking temperature through 3d magnetic exchange, Angew. Chem., Int. Ed. Engl. 52 (2013) 12014, https://doi.org/10.1002/anie.201306329.

[19] S.K. Langley, C. Le, L. Ungur, B. Moubaraki, B.F. Abrahams, L.F. Chibotaru, K.S. Murray, Heterometallic 3d–4f single-molecule magnets: Ligand and metal ion influences on the magnetic relaxation, Inorg. Chem. 54 (2015) 3631, https://doi.org/10.1021/acs.inorgchem.5b00219.

[20] S.K. Langley, N.F. Chilton, L. Ungur, B. Moubaraki, L.F. Chibotaru, K.S. Murray, Heterometallic tetranuclear [$Ln_2^{III}Co_2^{III}$] complexes including suppression of quantum tunneling of magnetization in the [$Dy_2^{III}Co_2^{III}$] single molecule magnet, Inorg. Chem. 51 (2012) 11873, https://doi.org/10.1021/ic301784m.

[21] S.K. Langley, D.P. Wielechowski, V. Vieru, N.F. Chilton, B. Moubaraki, L.F. Chibotaru, K.S. Murray, Modulation of slow magnetic relaxation by tuning magnetic exchange in Cr_2Dy_2 single molecule magnets, Chem. Sci. 5 (2014) 3246, https://doi.org/10.1039/c4sc01239a.

[22] S.K. Langley, D.P. Wielechowski, V. Vieru, N.F. Chilton, B. Moubaraki, L.F. Chibotaru, K.S. Murray, The first 4d/4f single-molecule magnet containing a Ru $(III)_2Dy(III)_2$ core, Chem. Commun. 51 (2015) 2044, https://doi.org/10.1039/c4cc08811e.

[23] G. Peng, Y.Y. Zhang, Z.Y. Li, G.E. Kostakis, First examples of polynuclear lanthanide diethyleneglycol-based coordination clusters, Eur. J. Inorg. Chem. 2017 (2017) 2700, https://doi.org/10.1002/ejic.201700168.

[24] (a) G.M. Sheldrick, Crystal structure refinement with SHELXL, Acta Crystallogr. Sect. C Struct. Chem. 71 (2015) 3, https://doi.org/10.1016/0097-8485(78)87001-6;
(b) O.V. Dolomanov, L.J. Bourhis, R.J. Gildea, J.A.K. Howard, H. Puschmann, OLEX2: A complete structure solution, refinement and analysis program, J. Appl. Chem. 42 (2009) 339.

[25] G.M. Sheldrick, SHELXT – Integrated space-group and crystal-structure determination, Acta Crystallogr. Sect. A Found. Adv. 71 (2014) 3, https://doi.org/10.1107/S2053273314026370.

[26] S.F.M. Schmidt, C. Koo, V. Mereacre, J. Park, D.W. Heermann, V. Kataev, C.E. Anson, D. Prodius, G. Novitchi, R. Klingeler, A.K. Powell, A three-pronged attack to investigate the electronic structure of a family of ferromagnetic Fe_4Ln_2 cyclic coordination clusters: a combined magnetic susceptibility, high-field/high-frequency electron paramagnetic resonance and [57]Fe Mössbauer study, Inorg. Chem. 56 (2017) 4796, https://doi.org/10.1021/acs.inorgchem.6b02682.

[27] A. Baniodeh, N. Magnani, Y. Lan, G. Buth, C.E. Anson, J. Richter, M. Affronte, J. Schnack, A.K. Powell, High spin cycles: topping the spin record for a single molecule verging on quantum criticality, NPJ Quantum Mater. 3 (2018) 10, https://doi.org/10.1038/s41535-018-0082-7.

[28] I.A. Kühne, N. Magnani, V. Mereacre, W. Wernsdorfer, C.E. Anson, A.K. Powell, An octanuclear $Cu(II)_4Dy(III)_4$ coordination cluster showing single molecule magnet behaviour from field accessible states, Chem. Commun. 50 (2014) 1882, https://doi.org/10.1039/c3cc46458j.

[29] J. Long, F. Habib, P.H. Lin, I. Korobkov, G. Enright, L. Ungur, W. Wernsdorfer, L.F. Chibotaru, M. Murugesu, Single-molecule magnet behavior for an antiferromagnetically superexchange-coupled dinuclear dysprosium(III) complex, J. Am. Chem. Soc. 133 (2011) 5319, https://doi.org/10.1021/ja109706y.